Theor Chem Acc (2002) 107:71–79
DOI 10.1007/s00214-001-0305-y

Theoretical
Chemistry Accounts

Regular article

Local-orbital-based correlated ab initio band structure calculations in insulating solids: LiF

Martin Albrecht

Laboratory of Applied Physics, Faculty of Engineering, Gunma University, Kiryu-shi, Gunma-ken, Tenjin-cho 1-5-1, 376-8515 Japan

Received: 25 June 2001 / Accepted: 31 August 2001 / Published online: 19 December 2001

Abstract. A local-orbital-based ab initio approach to calculate correlation effects on quasi-particle energies in insulating solids is presented. The use of localized Wannier-type Hartree–Fock orbitals allows correlation effects to be efficiently assessed. First a Green's function approach based on exact diagonalization is introduced and this is combined with an incremental scheme, while subsequently different levels of perturbative approximations are derived from the general procedure. With these methods the band structure of LiF is calculated and good agreement with experiment is found. By comparing the different approximations proposed, including the exact diagonalization procedure, their relative quality is established.

Key words: Wannier-type localized orbitals – Electron correlation – Ab initio band structure – Quasi-particle energies – Incremental scheme

1 Introduction

The present work introduces a new scheme for ab initio band structure calculations including correlation effects. Up to the present, such calculations are still subject to immense numerical efforts. A very efficient scheme is density-functional theory (DFT) [1, 2], which focuses on the electron density in order to obtain ground-state properties. In several cases the interpretation of the single orbital energies, retrieved in the self-consistent process, as quasi-particle energies also turns out to be successful. Particular attention has been paid to the local density approximation (LDA) to DFT, owing to its numerical feasibility; however, it is found that in insulating materials the LDA results tend to underestimate the band gap [3]. Improvements such as the GW approximation [4] or the optimized effective potential method [5] are available. A noteworthy improvement, using an exact exchange potential, has been presented by Städele et al. [6]. Yet all these procedures rely on special functionals which might not be improvable in a systematic way.

On the other hand, explicitly wave-function-based approaches, which are well explored in quantum chemistry, use a correlation interaction scheme to incorporate correlation effects and are hard to apply to solids owing to high numerical costs. They are, however, systematically improvable. Naturally, the first applications to infinite periodic systems focused on one-dimensional problems, i.e. polymers. Sun and Bartlett [7], Liegener [8], Bogár and Ladik [9] and Suhai [10] presented perturbative schemes, while Förner et al. [11] introduced a coupled-cluster method. Abdurahman et al. [12] obtained correlation corrections from an effective Hamiltonian.

Early proposals for three-dimensional applications date back to the use of local operators by Horsch et al. [13]. An ab initio approach based on local Hartree–Fock (HF) orbitals was introduced by Stoll [14], who set up an incremental scheme of rapidly decreasing correlation contributions to the ground-state energy. Gräfenstein et al. [15, 16] were able to extend this scheme to excitation energies, but using a finite-cluster approximation this attempt was restricted to the valence bands only when aiming at covalent semiconductors [17]. Recently, Tatewaki [18] presented a finite-cluster approximation for the case of LiF. In order to obtain genuine local HF orbitals for gap materials, taking into account the entire infinite system, Shukla et al. [19, 20] developed the program package WANNIER and also performed Ground-state correlation calculations [21]. The author of the present work proposed constructing an ab initio effective Hamiltonian perturbatively using such local HF orbitals [12, 22]. Igarashi et al. [23] conceived a local Green's function approach, which involves exact diagonalization of a model Hamiltonian in a selected subspace, and Takahashi and Igarashi [24, 25] applied this procedure to various open-shell crystals. This procedure was recently carried over to the ab initio case, where the use of the aforementioned incremental scheme allowed the necessary boost in numerical efficiency. Its feasibility was demonstrated by a modest basis set calculation on LiH [26].

In the present work this ab initio Green's function scheme is applied to LiF, which is the focus of recent state-of-the-art band structure calculations [18, 27]. Additionally, various perturbative approximations are derived from this scheme and the quality of the results is compared. The work is organized as follows. The Green's function approach and its combination with an incremental scheme are introduced in Sect. 2. Furthermore, perturbative variants are also presented. The results obtained for LiF are discussed in Sect. 3 and the conclusions are summarized in Sect. 4.

2 Theory

HF calculations are used as a starting point of many quantum chemical methods in order to address correlations. For the solid the HF band structure calculation can nowadays routinely be performed in reciprocal space, thus exploiting the translational invariance of periodic systems, for example, using the program package CRYSTAL [28], however, this results in extended Bloch states for the one-particle orbitals. The correlation hole around a quasi-particle, on the other hand, can be considered to have a fairly local nature [29]. In order to exploit this feature for the sake of feasible numerical efforts it seems advantageous to formulate the correlation corrections in terms of localized rather than extended HF orbitals. In this work the program package WANNIER, recently developed by Shukla et al. [19] was employed to obtain localized HF orbitals. This has been done routinely before [19–21] and is not described in the present work.

In the localized orbital basis an incremental scheme can be formulated for a variety of quantities in order to systematically include an increasing number of correlations. This scheme is applied to the self-energy in real space as explained in Sect. 2.1. The use of local HF orbitals allows separate regions characterized by strong, weak and very weak individual correlation contributions to the self-energy to be defined. For the strong contributions an exact diagonalization method is used, while further approximations are adequate for the weak parts. This approach is guided by the general idea of employing methods of different accuracy for different classes of correlation contributions as is efficiently done for molecules [30] as well as in an earlier application to LiH [26].

2.1 A Green's function approach

A Green's function approach was introduced by Igarashi et al. [23] and was applied to a Hubbard-type model Hamiltonian in several applications [24, 25]. Recently an ab initio calculation was performed for LiH [26]. In this section the description of the Green's function method is repeated. Additionally, several approximation schemes are introduced in Sect. 2.2.

The starting point of our correlation calculation is Wannier-type localized HF orbitals, referred to henceforth as local HF orbitals. At the HF level, a hole can be represented as

$$\|\mathbf{R}n\rangle = c_{\mathbf{R}n}|\Phi_{\mathrm{HF}}\rangle \ , \tag{1}$$

where $c_{\mathbf{R}n}$ destroys one electron in a local occupied HF orbital which is characterized by its unit cell, $\mathbf{R}$, and its cell orbital index, n. A similar description holds for the creation of an electron in a local HF orbital.

The Hamiltonian is partitioned into a zero-order Hamiltonian and a residual interaction using local HF orbitals and introducing compound indices $i = \mathbf{0}n, j = \mathbf{R}m$:

$$H = H_0 + W \tag{2}$$

$$H_0 = \sum_{ij} F_{ij} a_i^\dagger a_j \tag{3}$$

$$W = \sum_{ijkl} W_{ijkl} a_i^\dagger a_j^\dagger a_l a_k - \sum_{ij} \sum_{l}^{\mathrm{occ}} (W_{lilj} - W_{lijl}) a_i^\dagger a_j \ , \tag{4}$$

where F is the Fock operator and the residual interaction comprises the two-body part of the Coulomb interaction.

So far the compound indices $i = \mathbf{0}n, j = \mathbf{R}m$ have been used. Henceforth the cell vector is made explicit again. The Green's function is defined as

$$G_{nm}(\mathbf{R}, t) = -i\langle T[a_n(\mathbf{0}, 0) a_m^\dagger(\mathbf{R}, t)]\rangle \ , \tag{5}$$

where T is the time-ordering operator and the angled brackets denote the average over the exact ground state. By means of a space–time Fourier transform the Green function can be translated into reciprocal and frequency space, where it obeys the Dyson equation:

$$G_{nm}(\mathbf{k}, \omega) = G^0_{nm}(\mathbf{k}, \omega) + \sum_{kl} G^0_{nk}(\mathbf{k}, \omega) \Sigma_{kl}(\mathbf{k}, \omega) G_{lm}(\mathbf{k}, \omega) \ . \tag{6}$$

The indices n, m, k and l are used to denote both occupied and virtual orbitals. The Dyson equation (Eq. 6) introduces the self-energy $\Sigma_{kl}(\mathbf{k}, \omega)$, which contains the correlation effects. $G^0_{nm}(\mathbf{k}, \omega)$ is the HF propagator

$$\left[G^0(\mathbf{k}, \omega)\right]^{-1}_{nm} = \omega - F_{nm}(\mathbf{k}) \ . \tag{7}$$

As a result of Dyson's equation the Green function is then calculated from

$$G_{nm}(\mathbf{k}, \omega) = \left[\omega - F(\mathbf{k}) - \Sigma(\mathbf{k}, \omega)\right]^{-1}_{nm} \ . \tag{8}$$

The correlated band structure is given by the poles of the Green's function, which are numerically iteratively retrieved as the zeros of the denominator in Eq. (8).

The self-energy is approximated by decomposition into a retarded and an advanced part,

$$\Sigma_{kl}(\mathbf{k}, \omega) = \Sigma^{(\mathrm{r})}_{kl}(\mathbf{k}, \omega) + \Sigma^{(\mathrm{a})}_{kl}(\mathbf{k}, \omega) \ . \tag{9}$$

Furthermore, the configuration space is restricted to single excitations, i.e. three-body interactions.

In the following only the construction of the retarded self-energy part is given, the case of the advanced part being analogous. Returning to compound indices in real space, the indices now contain again both the lattice vector of the unit cell, the orbital number in this cell and

the spin. Let a, b, c and d and r, s, t and u represent occupied and virtual orbitals, respectively. The space of two-particle one-hole states (2p1h) is spanned by

$$|r,s,a\rangle = a_r^\dagger a_s^\dagger a_a |\Phi_{\mathrm{HF}}\rangle \ . \tag{10}$$

The Hamiltonian is in this basis

$$\begin{aligned}[\mathbf{H}^{\mathrm{R}}]_{rsa,r's'a'} &= \langle r,s,a|H-E_0|r',s',a'\rangle \\ &= \Gamma(rs;r's')\delta_{aa'} - F_{aa'}(\delta_{ss'}\delta_{rr'} - \delta_{rs'}\delta_{sr'}) \\ &\quad - \Gamma(sa';s'a)\delta_{rr'} + F_{rr'}\delta_{aa'}\delta_{ss'} \\ &\quad - \Gamma(ra';r'a)\delta_{ss'} + F_{ss'}\delta_{aa'}\delta_{rr'} \\ &\quad + \Gamma(ra';s'a)\delta_{sr'} - F_{sr'}\delta_{aa'}\delta_{rs'} \\ &\quad + \Gamma(sa';r'a)\delta_{rs'} - F_{rs'}\delta_{aa'}\delta_{r's} \ . \end{aligned} \tag{11}$$

The superscript R is used again to refer to the retarded part, meaning in this case that the matrix $\mathbf{H}^{\mathrm{R}}$ is set up in the 2p1h space. There is a similar equation for the 2h1p space. Γ is given by

$$\Gamma(rs;ta) = W_{rsta} - W_{rsat} \ . \tag{12}$$

Here E_0 is the HF ground-state energy, while the angled brackets now indicate the HF average.

Diagonalizing the matrix $\mathbf{H}^{\mathrm{R}}$ results in the eigenvectors $\mathbf{S}^{\mathrm{R}}$ and eigenvalues λ^{R}. The retarded part of the self-energy is then constructed as

$$\begin{aligned}\Sigma_{nm}^{(r)}(\mathbf{R},\omega) &= \sum_{rsa;r's'a'} \Gamma(rs;na) \\ &\quad \times \left[\omega - \mathbf{H}^{\mathrm{R}} + i\delta\right]^{-1}_{rsa;r's'a'} \Gamma(r's';ma') \\ &= \sum_{rsa;r's'a'} \Gamma(rs;na) \sum_q \mathbf{S}^{\mathrm{R}}_{rsa;q} \\ &\quad \times \frac{1}{\left(\omega - \lambda_q^{\mathrm{R}} + i\delta\right)} \mathbf{S}^{\mathrm{R}}_{q;r's'a'} \Gamma(r's';ma') \ . \end{aligned} \tag{13}$$

The translational invariance of the solid allows the index n in Eq. (13) to be confined to the central unit cell $\mathbf{0}$, while the index m is in unit cell $\mathbf{R}$ which has been made explicit. In the following the frequency dependence will also be indicated explicitly. The self-energy in reciprocal space, as it appears in Eq. (8), can then be obtained as a Fourier transformation:

$$\Sigma_{nm}^{(r)}(\mathbf{k},\omega) = \sum_{\mathbf{R}} \mathrm{e}^{i\mathbf{k}\mathbf{R}} \Sigma_{nm}^{(\mathrm{r})}(\mathbf{R},\omega) \ . \tag{14}$$

In principle, the three-body excitations $|r,s,a\rangle, |r',s',a'\rangle$ taken into account while performing the calculation should run over the entire solid. Secondly, Eq. (13) ought to be evaluated for each lattice vector $\mathbf{R}$ as all these terms are needed in Eq. (14); however, owing to the use of local HF orbitals, both infinite summations can be rendered finite. Since the correlation hole around a quasi-particle is for its major part a rather local quantity, it turns out that only excitations in the neighborhood of the central unit cell will considerably contribute to the self-energy, so the number of relevant three-body excitations is finite. Secondly, by the same token the parts of the self-energy with $\mathbf{R} \neq \mathbf{0}$ will be found to decay rapidly with increasing distance of $\mathbf{R}$, so again only a finite number of calculations need to be performed. Yet it might turn out that still a rather large environment around a quasi particle is needed and the task of diagonalizing this part might still exceed computational power. To address this point, an incremental scheme was introduced by Stoll [14] for the ground-state energy and was later adapted to the case of quasi-particle energies by Gräfenstein et al. [15, 16]. The idea amounts to breaking up the task of diagonalizing the Hamiltonian in the full space of configuration interaction (here, e.g. three-body interaction) into a series of smaller tasks arranged in a controlled and well-defined way. This has been described in detail in Ref. [26] and is briefly reviewed in the following.

The compound indices $i = \mathbf{0}n, i' = \mathbf{0}m$, and $j = \mathbf{R}m$ are used again, while the retardation index of the self-energy together with the frequency dependence is suppressed. Let us first look at the on-site part of the self-energy, i.e. the part with $\mathbf{R} = \mathbf{0}$ in Eq. (13). To calculate the matrix element $\Sigma_{ii'}$ from Eq. (13), a first simple approximation is introduced by restricting all excitations, i.e. all indices r, s, a and r', s', a' in Eq. (13) to the central unit cell $\mathbf{0}$. This is sketched in the left panel of Fig. 1, labeled intra. The figure shows a certain finite environment of the solid around the central unit cell and displays by continuous shading the active cells where excitations are taken into account. Let us denote the result of this simple procedure by $\Sigma_{ii';\mathbf{0}}$. Then, this result can be defined to be the first of a series of approximations to the exact result obtained from correlating the entire solid. Since only excitations in the central cell were allowed, it is called the intra increment, defined as:

$$\Delta\Sigma_{ii'}^{\mathrm{intra}} = \Sigma_{ii';\mathbf{0}} \ . \tag{15}$$

The next step is to perform a calculation of the self-energy where now excitations are allowed in the central

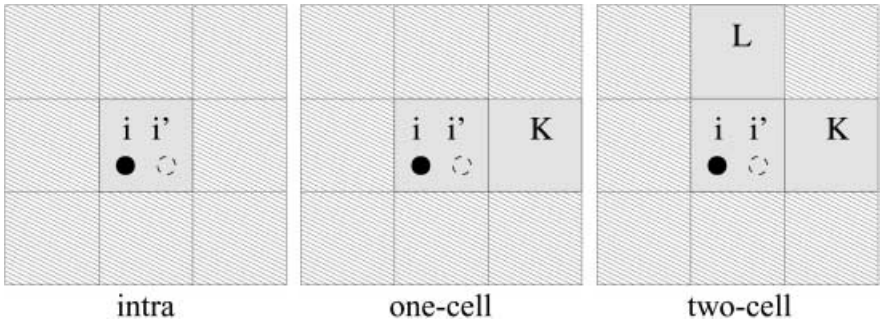

Fig. 1. Each of the three panels shows the same finite nine-cell part of the infinite solid. The active cells are displayed schematically for an intra cell correlation calculation (“intra”), a one-cell increment and a two-cell increment (denoted by “one-cell” and “two-cell”, respectively). As indicated, orbitals i and i' are in the same unit cell

cell and one additional cell, denoted K in the middle panel of Fig. 1. Denoting the result of this calculation as $\Sigma_{ii';\mathbf{R}_K}$, the corresponding one-cell increment, labeled I to mark the use of one additional cell, which gives the effect of this additional cell K on the self-energy, is defined to be

$$\Delta\Sigma^{\mathrm{I}}_{ii';\mathbf{R}_K} = \Sigma_{ii';\mathbf{R}_K} - \Delta\Sigma^{\mathrm{intra}}_{ii'} \quad . \tag{16}$$

Obviously this procedure can be continued to include more and more cells. As a last example, the two-cell increment, labeled II, indicated on the right of Fig. 1, is given by

$$\Delta\Sigma^{\mathrm{II}}_{ii';\mathbf{R}_K\mathbf{R}_L} = \Sigma_{ii';\mathbf{R}_K\mathbf{R}_L} - \Delta\Sigma^{\mathrm{I}}_{ii';\mathbf{R}_K} - \Delta\Sigma^{\mathrm{I}}_{ii';\mathbf{R}_L} - \Delta\Sigma^{\mathrm{intra}}_{ii'} \quad . \tag{17}$$

The self-energy is finally approximated by

$$\Sigma_{ii'} = \Delta\Sigma^{\mathrm{intra}}_{ii'} + \sum_{\mathbf{R}_K} \Delta\Sigma^{\mathrm{I}}_{ii';\mathbf{R}_K} + \frac{1}{2!} \sum_{\mathbf{R}_K \neq \mathbf{R}_L} \Delta\Sigma^{\mathrm{II}}_{ii';\mathbf{R}_K\mathbf{R}_L} + \cdots \quad . \tag{18}$$

Of course, there are an infinite number of one-cell, two-cell and higher-order increments; however, as pointed out earlier, only a limited number of them need actually to be calculated since with increasing number of active cells and the distance between them the respective increments rapidly decay to zero. As the decrease of the increments can be monitored, the truncation of the summation (Eq. 18) can be controlled explicitly. All this effort amounts to calculating what might be called the $\mathbf{R} = \mathbf{0}$ part or the on-site part of the self-energy, i.e.

$$\Sigma_{ii'} = \Sigma_{nm}(\mathbf{0}) \quad . \tag{19}$$

To be specific, increments with cells arranged approximately as a sphere in a certain range, R_c will be calculated explicitly. Beyond R_c individual contributions are found to basically vanish and only the sum up to infinity would give a noticeable contribution, well known as the long-range polarization cloud. As has been demonstrated in earlier works [15–17, 26], this part can be well approximated by a continuum correction. To this end the polarization effect of the part of the solid outside the sphere that has been taken into account explicitly so far is taken to be that of a dielectric continuum and is a constant. So the part of the sum in Eq. (18) which involves cells with lattice vectors $|\mathbf{R}_{K,L,\ldots}| > R_c$ is approximated by a constant, leading to a constant shift of the bands towards the Fermi level.

To obtain the on-site part of the self energy Eq. (19), a series of calculations for as many individual increments in the sum (Eq. 18) as necessary is performed.

As described in Ref. [26], the self-energy matrices with $\mathbf{R} \neq \mathbf{0}$ can be obtained in the same way. Naturally the same series of increments as in Eqs. (15), (16), (17), and (18) can be calculated for each $\mathbf{R} \neq \mathbf{0}$, giving rise to what might be referred to as the nonlocal terms of the self-energy, by means of the following completely analogous increments:

$$\begin{aligned}
\Delta\Sigma^{\mathrm{intra}}_{ij} &= \Sigma^0_{ij} \\
\Delta\Sigma^{\mathrm{I}}_{ij;\mathbf{R}_K} &= \Sigma_{ij;\mathbf{R}_K} - \Delta\Sigma^{\mathrm{intra}}_{ij} \\
\Delta\Sigma^{\mathrm{II}}_{ij;\mathbf{R}_K\mathbf{R}_L} &= \Sigma_{ij;\mathbf{R}_K\mathbf{R}_L} - \Delta\Sigma^{\mathrm{I}}_{ij;\mathbf{R}_K} - \Delta\Sigma^{\mathrm{I}}_{ij;\mathbf{R}_L} - \Delta\Sigma^{\mathrm{intra}}_{ij} \\
\Sigma_{ij} &= \Delta\Sigma^{\mathrm{intra}}_{ij} + \sum_{\mathbf{R}_K} \Delta\Sigma^{\mathrm{I}}_{ij;\mathbf{R}_K} + \frac{1}{2!} \sum_{\mathbf{R}_K \neq \mathbf{R}_L} \Delta\Sigma^{\mathrm{II}}_{ij;\mathbf{R}_K\mathbf{R}_L} + \cdots \quad ,
\end{aligned} \tag{20}$$

where orbital i resides in cell $\mathbf{0}$ and j in cell $\mathbf{R}$. The simplest increment, the "intra cells" increment is obtained from a calculation of the self-energy in which only three-body excitations in the two cells $\mathbf{0}$ and $\mathbf{R}$, where the orbitals i and j reside, are permitted. It is labeled Σ^0_{ij} in the Eq. (20). Higher-order increments are obtained by allowing more and more cells to be active and finally Eq. (20) leads to the $\mathbf{R}$-dependent parts of the self-energy, i.e.

$$\Sigma_{ij} = \Sigma_{nm}(\mathbf{R}) \quad . \tag{21}$$

2.2 Perturbative approximations

Up to now it has been shown how the use of local HF orbitals can allow for an efficient calculation of the self-energy. However, the numerical effort for the diagonalization of the Hamiltonian in the space of three-body interactions (Eq. 11) is considerable even for a small number of active cells. Since the diagonalization is the most expensive step, it sets the overall scaling of the method and is thus similar to a singles configuration interaction procedure (SCI). A straightforward implementation scales with L^3 if the matrix is of size $L \times L$. For single excitations L scales as $V(V-1)O \approx V^2O$ if V and O are the numbers of virtual and occupied orbitals per unit cell, respectively. Since there is no general reason to assume a strong scaling of the number of increments and cells per increment to be taken into account with the number of basis functions per unit cell or the number of atoms per unit cell, the latter are the decisive quantities, so the method scales as V^6O^3. It is the same scaling as that of a straightforward SCI. However, this steep increase in numerical effort with the size of the basis functions has not prevented large-scale molecular SCI and even single and doubles configuration interaction calculations, so efficient approximations to the diagonalization have been devised and could be used for the present case as well. Another alternative is presented by perturbative schemes which scale linearly in L or as V^2O. Along with the exact diagonalization presented so far, perturbative schemes were tested in addition. They are all derived from the procedure put forth so far and can be easily accommodated in the general program package.

A general perturbative approximation is obtained by skipping the diagonalization of the Hamiltonian matrix (Eq. 11) and just retaining its diagonal as eigenvalues. This immediately transforms Eq. (13) for the retarded part of the self-energy into the second-order expression

$$\Sigma^{(r)}_{nm}(\mathbf{R},\omega) \approx \sum_{rsa} \Gamma(rs;na)\frac{1}{\left(\omega - \lambda^{\mathrm{R}}_{rsa} + i\delta\right)}\Gamma(rs;ma) \ , \tag{22}$$

where $\lambda^{\mathrm{R}}_{rsa}$ are the aforementioned diagonal elements of the full Hamiltonian (Eq. 11).

$$\begin{aligned}\lambda^{\mathrm{R}}_{rsa} &= F_{rr'} + F_{ss'} - F_{aa'} + \Gamma(rs;rs) - \Gamma(ra;ra) - \Gamma(sa;sa) \\ &= \epsilon_r + \epsilon_s - \epsilon_a + J_{rs} - K_{rs} \\ &\quad - Jra + K_{ra} - Jsa + K_{sa} \ .\end{aligned} \tag{23}$$

In the last line of Eq. (23) the Coulomb and exchange coefficients $J_{ij} = W_{iijj}$, and $K_{ij} = W_{ijji}$ were used together with the abbreviation $\epsilon_i = F_{ii}$. The result (Eqs. 22, 23) is well known as the Epstein–Nesbet approximation [31]. It results from retaining the diagonal of the full Hamiltonian in the configuration space. A second point of view is discussed later. Of course the usual second-order perturbation theory can be derived from Eq. (22) just by replacing the diagonal elements (Eq. 23) with the matrix elements of the Fock matrix only, i.e.

$$\lambda^{\mathrm{R}}_{rsa} = \epsilon_r + \epsilon_s - \epsilon_a \ . \tag{24}$$

Equation (22) together with the ordinary energy denominator (Eq. 24) yield the self-energy used by Liegener [8] and Bogàr and Ladik [9] in their band structure calculation of polymers. It has been pointed out that the difference between Eqs. (23) and (24) can also be understood in terms of second-order diagrams [31]. By depicting the second-order self-energy as obtained with the energy denominator given by Eq. (24) as a bare second-order diagram, the solution (Eq. 23) is obtained as a summation of special higher-order diagrams up to infinite order. This is depicted in Fig. 2. The left-hand side of Fig. 2 represents a bare second-order Coulomb contribution to the self-energy matrix element $\Sigma^{(r)}_{mn}$ and reads

$$\frac{W_{nars}W_{mars}}{\omega + \epsilon_a - \epsilon_r - \epsilon_s + i\delta} \ . \tag{25}$$

On the right-hand side of the Fig. 2 a Coulomb insertion has been added with the incoming and outgoing indices chosen to be identical, giving a contribution

$$\frac{W_{nars}W_{mars}}{\omega + \epsilon_a - \epsilon_r - \epsilon_s + i\delta}J_{rs} \ . \tag{26}$$

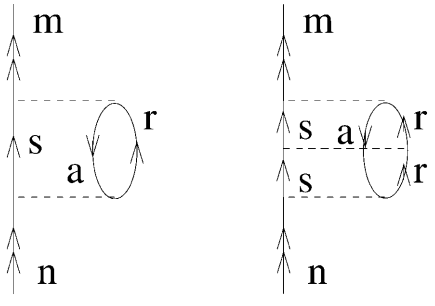

Fig. 2. Second- and third-order diagrams corresponding to the contributions (Eqs. 25, 26) to the self-energy matrix element $\Sigma^{(r)}_{nm}$

Adding more and more such insertions and adding all contributions yields a power series in J_{rs} which can be written by just adding a $-J_{rs}$ to the bare energy denominator of Eq. (25). By analogy, the remaining additional Coulomb and exchange terms can be derived in the Epstein–Nesbet expression (Eq. 23).

At this stage it is to be noticed that the self-energy is still frequency-dependent. This means that while iterating on ω in Eq. (8) to find the poles of the Green's function, the procedure has to go through all of the increments used in Eqs. (18) and (20) in each step. While this is practical for the limited number of on-site increments, it is less feasible for all increments, particularly those describing the $\mathbf{R} \neq \mathbf{0}$ part of the self-energy. Fortunately, there is an elegant solution to the problem by fixing the frequency so that Eq. (13) or Eq. (22) takes the second-order form:

$$\Sigma^{(\mathrm{r})}_{nm}(\mathbf{R} \neq \mathbf{0}) \approx \sum_{rsa} \Gamma(rs;na)\frac{1}{(\epsilon_n + \epsilon_a - \epsilon_r - \epsilon_s)}\Gamma(rs;ma) \ . \tag{27}$$

It has been shown in an earlier work [26] that this particular approximation amounts to calculating an effective Hamiltonian, which puts the approximation (Eq. 27) into the light of a well-defined context. Details of the effective Hamiltonian treatment can be found in a previous article, where this procedure was applied to ring systems [22]. Further applications have been done for polymers [12]. Equation (27) is suitable for a further discussion of what processes are included in the three-body-scattering theory. As long as the conduction bands are considered, the indices n and m of the retarded self-energy matrix, $\Sigma^{(\mathrm{r})}_{nm}$, refer to particles and Eq. (27) can be represented as second-order diagrams of the type shown on the left side of Fig. 2. They clearly represent single excitations. However, in the case of valence-band calculations the indices n and m refer to holes and the retarded self-energy matrix (Eq. 27) is now represented by the two leftmost diagrams shown in Fig. 3. For $m \neq n$ the left diagram applies and displays a double excitation on top of the single hole coupling directly to the model space. For $m = n$ the ground-state correction diagram in the middle of Fig. 3 is obtained. So the direct coupling of

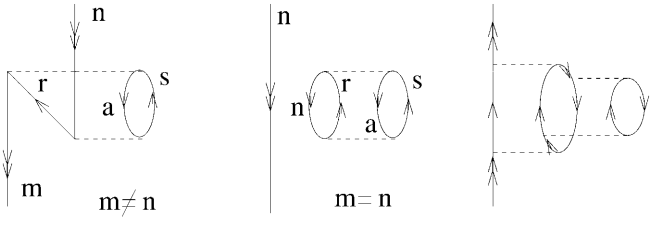

Fig. 3. Diagrams for $\Sigma^{(r)}_{nm}$ derived from Eq. (27) for the case where the orbitals n and m refer to holes instead of particles. The two diagrams to the left show the direct coupling of the double excitations to the model space and ground-state correlation corrections, respectively. The diagram on the right gives an example for the coupling of a double excitation to a single excitation and has been left unindexed

the doubles to the model space is included in the theory. For the conduction bands the advanced part of the self energy, $\Sigma^{(a)}_{nm}$, given by a formula similar to Eq. (27) takes the role of these two leftmost doubles diagrams in Fig. 3. However, since the Hamiltonian is only diagonalized in the subspace of single excitations, the coupling of the doubles to the singles is not taken into account. Since the omission of higher-order excitations might result in some fortuitous error cancellation, it would be desirable to know how large the effect of such excitations are in each case. The diagram on the right of Fig. 3 exemplifies such a double excitation which couples to a single excitation. The coupling of the doubles to the singles is at least fourth order and can thus be expected to be rather small, yet to estimate the error incurred by restricting the matrix (Eq. 11) to the single excitation space, the following diagonal dressing procedure is adopted. If the single excitation space is indexed with S and the double one with D, the procedure up to now can be symbolized by the eigenvalue problem

$$\mathbf{H}_{\mathrm{SS}}\mathbf{C}_{\mathrm{S}} = \lambda\mathbf{C}_{\mathrm{S}} \ , \tag{28}$$

where $\mathbf{H}_{\mathrm{SS}}$ is the matrix (Eq. 11) and $\mathbf{C}_{\mathrm{S}}$ is an eigenvector with eigenvalue λ. Taking into account single and double excitations the problem grows to

$$\begin{pmatrix} \mathbf{H}_{\mathrm{SS}} & \mathbf{H}_{\mathrm{SD}} \\ \mathbf{H}_{\mathrm{DS}} & \mathbf{H}_{\mathrm{DD}} \end{pmatrix} \begin{pmatrix} \mathbf{C}_{\mathrm{S}} \\ \mathbf{C}_{\mathrm{D}} \end{pmatrix} = \lambda \begin{pmatrix} \mathbf{C}_{\mathrm{S}} \\ \mathbf{C}_{\mathrm{D}} \end{pmatrix} \ . \tag{29}$$

Solving the second line for $\mathbf{C}_{\mathrm{D}}$ and inserting the result in the first line yields an effective Hamiltonian $\mathbf{H}^{\mathrm{eff}}_{\mathrm{SS}}$ which operates entirely in the space of the single excitations but incorporates the effects of the double excitations as well. Specifically one obtains:

$$\underbrace{\left[\mathbf{H}_{\mathrm{SS}} - \mathbf{H}_{\mathrm{SD}}[\mathbf{H}_{\mathrm{DD}} - \lambda]^{-1}\mathbf{H}_{\mathrm{DS}}\right]}_{\mathbf{H}^{\mathrm{eff}}_{\mathrm{SS}}} \mathbf{C}_{\mathrm{S}} = \lambda\mathbf{C}_{\mathrm{S}} \ . \tag{30}$$

The under-braced effective Hamiltonian, $\mathbf{H}^{\mathrm{eff}}_{\mathrm{SS}}$, depends on the sought eigenvalue, λ. A perturbative solution can be constructed as before by retaining only the diagonal h_{S} and h_{D} of $\mathbf{H}_{\mathrm{SS}}$ and $\mathbf{H}_{\mathrm{DD}}$ in Eq. (30). Without taking into account double excitations the eigenvalues λ would be identical with the diagonal elements h_{S}. The solutions to Eq. (30) can be found iteratively for each state, S, of single excitations by:

$$\lambda^{\mathrm{n}}_{\mathrm{S}} = \lambda^{\mathrm{n-1}}_{\mathrm{S}} - \sum_{\mathrm{D}} \frac{\mathbf{H}_{\mathrm{SD}}\mathbf{H}_{\mathrm{DS}}}{h_{\mathrm{D}} - \lambda^{n-1}_{\mathrm{S}}} \ , \tag{31}$$

$$\lambda^{0}_{\mathrm{S}} = h_{\mathrm{S}} \ , \tag{32}$$

$$h^{\mathrm{eff}}_{\mathrm{S}} = \lambda^{\infty}_{\mathrm{S}} \ . \tag{33}$$

The diagonal elements $h^{\mathrm{eff}}_{\mathrm{S}}$ of the matrix $\mathbf{H}_{\mathrm{SS}}$ then represent dressed elements incorporating the effects of double excitations; hence, the name diagonal dressing. Once they are obtained, the calculation proceeds as before in the single excitation space. Throughout the following calculations, only single excitations are taken into account. The diagonal dressing method is applied only once for a test calculation to assess the effect of double excitations.

3 Results and discussion

In this section the theory is applied to LiF. Recent HF calculations in localized Wannier–type orbitals were presented by Shukla et al. [20]. To incorporate correlation effects in the band structure, the LDA and the GW approximation have been applied recently [27] as well as a finite-cluster approach [18]. In the present work, localized HF orbitals are calculated as a starting point for the correlation procedure. This was done using the program package WANNIER [19]. A [4s3p1d] basis set was used for the fluorine anion, while a [2s1p] basis set was used for the lithium cation. While for the lithium atom this is a polarized single-zeta basis set, for the cation it constitutes a polarized double-zeta basis. This point has been carefully studied by Tatewaki [18], who showed that a [2s1p] basis set performs fine in the present case. The basis sets of Ref. [20, 36] were used with slight modifications in the exponents of the outer p orbitals, which were optimized for the solid case using WANNIER. The same holds for an additional d function provided for fluorine. The basis set is shown in Table 1.

All the calculations were done at the experimental face-centered-cubic lattice constant $a = 3.990$ Å with fluorine at the $(0, 0, 0)$ position and lithium at $(0, 0, a/2)$.

As an analysis of the mechanism of the incremental scheme, the importance of different increments is considered. Including or omitting an increment in the band structure calculation gives insight into the contribution of this very increment. In the upper part of Table 2 the contribution of various increments to the correlation correction of the fundamental gap at the Γ point is presented. All increments belong to the series (Eq. 18) of

Table 1. Basis set for the LiF calculation

	F		Li	
	Exponents (bohr^{-2})	Coefficients	Exponents (bohr^{-2})	Coefficients
1*s*	13770.000	0.000877	700.0	0.001421
	1589.000	0.009150	220.0	0.003973
	327.600	0.048600	70.0	0.016390
	91.460	0.169100	20.0	0.089954
	30.500	0.370700	5.0	0.315646
	11.460	0.416500	1.5	0.494595
	4.660	0.131600		
2*s*	19.290	−0.118300	0.5	1.0
	4.586	−0.127700		
	1.387	1.000		
3*s*	0.431	1.000		
4*s*	0.22	1.00		
2*p*	10.56917	0.126452	0.55	1.00
	2.19471	0.478100		
3*p*	0.47911	1.00		
4*p*	0.22	1.00		
3*d*	1.54	1.00		

Table 2. Individual increments as obtained with the Green's function method and their contribution to a narrowing of the Hartree–Fock (HF) gap in (eV) are depicted in the upper part. The indices 1, 2 and 3 indicate that the additional cells involved in the respective increments are within the first, the two first or the three first coordination spheres, respectively. *S* refers to one-cell increments, *D* to two-cell increments. The intra increment as obtained from various levels of approximation is analyzed in the lower part. The lines Green's, *EN*, *PT* and H_{eff} show the results obtained with the Green's function method, the Epstein–Nesbet approximation, perturbation theory and the effective Hamiltonian, respectively

		Closing of the gap
Increment (Green's)	Intra	5.654
	S_1	0.190
	S_2	0.032
	S_3	0.007
	D_1	0.002
Method (for intra)	Green's	5.654
	EN	5.547
	PT	4.984
	H_{eff}	3.598

the local part of the self-energy and were calculated using the Green's function method implying exact diagonalization. The intra increment gives by far the largest individual contribution, reducing the HF gap by 5.65 eV. The one-cell increments take into account excitations spread over the central cell and one additional cell. They are denoted as S_n in Table 2, were *n* indicates that the additional cell is chosen from the *n*th coordination sphere. Shifting the additional cell from a first-nearest-neighbor position (S_1) to a third-nearest one (S_3) decreases the one-cell contribution from 0.190 to 0.007 eV. This tiny contribution is already three orders of magnitude smaller than the intra increment. Even the largest two-cell increment, D_1, amounts to only 0.002 eV, which is 2 orders of magnitude smaller than its one-cell increment counterpart, S_1. The rapid decrease of increment contributions which manifests itself in Table 2 is a consequence of the fairly local character of a correlation hole around a quasi-particle. It allows the efficient calculation of the band structure including major correlation effects, provided local HF orbitals are used. In fact, all one-cell increments up to third-nearest neighbors have been taken into account. Similarly, the "intra cells" increments for the nonlocal part of the self-energy are taken into account in the same range. Since their contribution is found to be tiny, they are calculated perturbatively from an effective Hamiltonian (Eq. 27).

The numerically most expensive increment is the (least needed) D_1 double-cell increment which involves diagonalizing three unit cells at a time. It requires the diagonalization of a $10^4 \times 10^4$ matrix and takes some hours on a standard machine. Since efficient quantum chemistry molecular program packages diagonalize even much larger systems than the equivalent of Li_3F_3, adopting more efficient diagonalization schemes would also boost the method presented here. Additionally, the use of point group symmetries would significantly lower the costs. It can thus be assumed that numerically the approach of this work can be made feasible for a range of interesting crystals.

For the intra increment the results of the different approximations discussed in Sect. 2.2 are compared in the lower part of Table 2. The term "Green's function method" is used in this context to imply the exact diagonalization step and the subsequent construction of the self-energy according to Eq. (13). To obtain the second order Epstein–Nesbet (EN) results, Eq. (22) was used together with the energies (Eq. 23), as explained in Sect 2.2. The term "perturbation theory" refers to the use of Eq. (22) with the bare energies (Eq. 24). All these schemes lead to the final solution by iterating on the frequency, ω. The construction of a second-order effective Hamiltonian, on the other hand, follows Eq. (27). Clearly, the latter gives the poorest approximation, as can be seen by comparing the respective contribution in line H_{eff} in Table 2 with the result of the Green's function approach. Perturbation theory and the EN formulation yield results in between. In fact, the EN result is quite close to the result obtained by exact diagonalization, yielding an intra increment contribution of 5.547 eV, which differs little from the Green's function result of 5.654 eV. The same tendancy has been described in detail by Reinhardt and Malrieu [31] in their discussion of correlation contributions to the ground state of various ring systems. They pointed out that particle–hole lines in diagrams such as that on the right-hand side of Fig. 2 diminish the energy denominator via Eq. (23) and thus enhance the contribution of this diagram, while the opposite holds for particle–particle or hole–hole lines. It was further concluded that the overall balance leads the particle–hole contributions to dominate the summation, so the EN approximation yielded results which were close to nonperturbative ones when local HF orbitals were employed. Obviously in this work the same holds for the band structure and it can be argued in much the same way that there are more possibilities for particle–hole lines than for particle–particle lines in diagrams such as that on the right-hand side of Fig. 2. Finally, the effect of double excitations was estimated by repeating the calculation for the intra increment with the Green's function method while using a dressed-diagonal constructed from (Eq. 31). It was found that this leads only to a slight increase of 0.4% over the bare value of 5.654 eV. At least for the present system the effect of the doubles can thus be assumed to be rather small. This finding confirms an earlier, less approximate, analysis for the case of diamond [17]. Using an effective Hamiltonian and a finite-cluster approach, increments were calculated in three ways, namely, taking into account only single excitations in a strict sense (which is only diagrams of the type shown on the left of Fig. 2, i.e. only the retarded part of the self energy in Eq. 9), considering only double excitations (which means only diagrams such as the two leftmost ones in Fig. 3, i.e. in the present formulation only the advanced part of the self-energy in Eq. 9), and including the coupling between single and double excitations. It was reported that for diamond the intra increment of singles only plus doubles only amounts to 0.12136 Hartree, while the full calculation including the coupling

between singles and doubles (as indicated in the diagram on the right side of Fig. 3) yields 0.12366 hartree, which is an increase of just 1.9% .

For the band structure calculation the increments for the local part of the self-energy (Eq. 18) are calculated with the Green's function procedure from Eq. (13). The nonlocal part gives only a rather small contribution and its increments which appear in Eq. (20) are obtained from the perturbative expression (Eq. 27). The final result is shown in Fig. 4. The upper three valence bands due to the p orbitals at the fluorine sites as well as the lowest four conduction bands are depicted. The solid lines represent the HF result, while the dashed lines give the result of the correlation calculation. Additionally, some values of the bands at high symmetry **k** points are given in Table 3. The fundamental gap appears at the Γ point. Its HF value of 22.40 eV is by far too large when compared with experiment. This shortcoming is corrected by taking into account electron correlations. The calculation of this work leads to a gap of 13.50 eV, which amounts to a shrinking of the gap of 8.90 eV. This result compares well with the experimental value of 13.5 eV [32, 33]. Naturally, this should not lead to the conclusion that the method presented yields results with such a high accuracy, since there is some uncertainty in the measurements, some of which suggest a gap of 14.2 eV [34] as well as in the calculations, where the long-range-polarization part was approximated and contributes with 0.45 eV to the shrinking of the gap, i.e. with 5% . But the nice match found is nonetheless reassuring. A comparison with other ab initio calculations is shown in Table 4. Tatewaki [18] explored several approaches, two of which are stated in the table, the local density function (LDF) procedure and the embedded cluster approach, both with correlation corrections (labeled LDF and cluster in Table 4). The HF, LDA and GW results are taken from Ref. [27]. The correlated results are in a narrow range from the 13.5 eV of this work to 14.3 eV given by the GW calculation in Ref. [27], (except the LDA, which underestimates the gap with 8.82 eV), and are close to experiment. For the sake of comparison the gap was recalculated using the

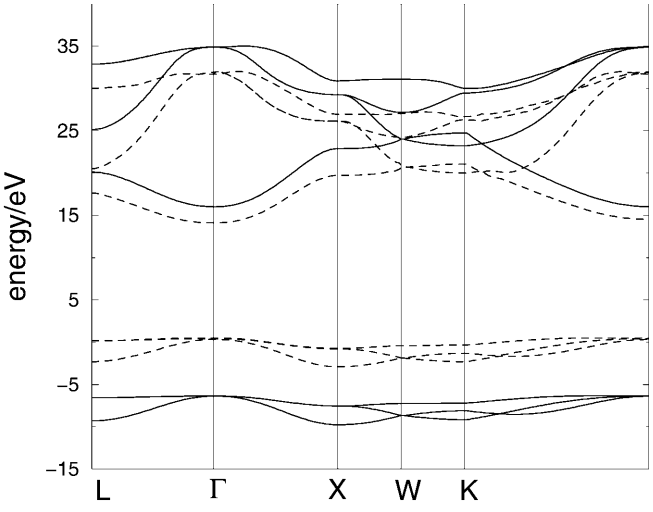

Fig. 4. Band structure of LiF for selected directions in the first Brillouin zone between $L[b(\frac{1}{2},\frac{1}{2},\frac{1}{2})]$, $\Gamma[(0,0,0)]$, $X[b(1,0,0)]$, $W[b(1,\frac{1}{2},0)]$ and $K[b(\frac{3}{4},\frac{3}{4},0)]$ (Cartesian coordinates, $b=\frac{2\pi}{a}$). The upper three valence bands together with the lowest four conduction bands are shown as solid and dashed lines for the Hartree–Fock and the correlated results, respectively

Table 3. Energy values (eV) of the upper three valence bands (v_1–v_3) and the lower three conduction bands (c_1–c_3) at the points $L[b(\frac{1}{2},\frac{1}{2},\frac{1}{2})]$, $\Gamma[(0,0,0)]$, $X[b(1,0,0)]$, $W[b(1,\frac{1}{2},0)]$ and $K[b(\frac{3}{4},\frac{3}{4},0)]$ (Cartesian coordinates, $b=2\pi/a$). Both the HF results as well as the correlated ones are given. In the last line the fundamental gap is stated

	L		Γ		X		W		K	
	HF	Corr	HF	Corr	HF	Corr	HF	Corr	HF	Corr
v_1	−9.30	−2.29	−6.39	0.49	−9.76	−2.90	−8.68	−1.87	−9.16	−2.29
v_2	−6.60	0.17	−6.39	0.49	−7.55	−0.74	−8.68	−1.87	−8.12	−1.30
v_3	−6.60	0.17	−6.39	0.49	−7.55	−0.74	−7.27	−0.43	−7.21	−0.34
c_1	20.11	17.75	16.01	13.99	22.88	19.40	23.99	20.43	23.21	19.99
c_2	25.13	20.11	34.88	31.88	29.27	25.74	23.99	20.43	24.72	20.66
c_3	32.87	29.99	34.88	31.88	29.27	25.74	27.17	24.53	29.44	25.96
Gap			22.40	13.50						

Table 4. Comparison of values for the band gap and the valence band width from various calculations. The column labels are as explained in the text. Width refers to the valence band width. Experimental values are also given in the last two columns. All values are in electron volts

	This work			From Ref. [18]		From Ref. [27]			Exp
	HF	H_{eff}	Corr	LDF	Cluster	HF	LDA	GW	
Gap	22.40	17.30	13.50	13.9	13.9	21.29	8.82	14.30	13.5[a] 14.2[b]
Width	3.37		3.40	2.8	2.7	3.31	3.12	3.61	3.5[c]

[a] From Ref. [32, 33]
[b] From Ref. [34]
[c] From Ref. [35]

second-order effective Hamiltonian expression (Eq. 27) for all increments, i.e. also for the local part of the self-energy in Eq. (18). It is found to be 17.3 eV as can be seen from column $\mathbf{H}_{\text{eff}}$ in Table 4. While this gives a considerable correlation correction to the HF gap, it falls short of fully accounting for the narrowing of the HF gap to 13.5 eV.

Secondly the width of the three upper valence bands is compared. While the usual tendency to be expected is a flattening of the bands, in the case of the LiF valence bands this effect is not pronounced. In the present calculation the HF band width of 3.37 eV basically does not change, displaying a minute broadening to 3.40 eV. This again, however, matches with the experimental width of 3.5 eV [35]. Also, the other works cited in Table 4 consistently show the same tendency. Tatewaki observed a slight broadening of his self-consistent-field value of 2.7 eV (not quoted in the table) to 2.8 eV obtained with the LDF method. His cluster approach does not change the width at all, leaving it at 2.7 eV. By the same token Shirley [27] found a HF width of 3.31 eV, which is somewhat smaller than the correlated value of his GW result (3.61 eV). So both the tendency and the magnitude of the valence band width of this work are consistent with other calculations and with experiment. Tatewaki [18] also pointed out that there is a more recent experiment giving a much larger width of 6.1 or even 10.5 eV [32], but argues convincingly that an enhanced sensitivity is likely to have recorded impurity effects.

4 Conclusion

In conclusion a localized-orbital-based ab initio scheme for band structure calculations which is designed to include correlation effects on top of HF results has been presented. The procedure starts from localized HF orbitals and strives to calculate the self-energy matrix. This task was efficiently split into the calculation of individual increments arranged in a series of rapidly decaying contributions. The scheme is flexible and allows a different treatment for different contributions, depending on their relative weight. Several perturbative formulations were retrieved from the Green's function scheme and were easily incorporated in the program. Their respective level of accuracy was found to be close to earlier findings. The results for LiF match with experiment and are consistent with other most recent state-of-the-art methods. Being explicitly orbital-based, the scheme presented is amenable to systematic improvements in a clear manner. This is because the applied method, i.e. exact diagonalization, is already exact, so taking into account double excitations, triple excitations, etc. yields a hierarchy of calculations leading to full configuration interaction. This, as well as taking into account larger basis sets and more increments in principle does not imply changes to the scheme and its formulas, so one has a clear prescription of how to proceed. In practice, of course, enlarging the basis set or taking into account higher-order excitations leads to a steep increase in the size of the matrix to be diagonalized, so further approximations might be inevitable. An example has been given by means of the diagonal-dressing technique.

Acknowledgements. The author gratefully acknowledges the support of the Japan Society for the Promotion of Science, grant no. P99 757, and the Alexander von Humboldt foundation as well as calulation power provided by the Max Planck Institute for Physics of Complex Systems in Dresden, Germany.

References

1. Hohenberg P, Kohn W (1964) Phys Rev B 136: 864
2. Kohn W, Sham LJ (1965) Phys Rev A 141: 1133
3. Ching WY, Gan F, Huang M-Z (1995) Phys Rev B 52: 1596
4. Hott R (1991) Phys Rev B 44: 1057
5. Grabo T, Kreibich T, Kurth S, Gross EKU (1998) In: Anisimou VI (ed) Strong Coulomb correlations in electronic structure: beyond the local density approximation. Gordon & Breach, London
6. Städele M, Moukara M, Majewski JA, Vogl P, Görling A (1999) Phys Rev B 59: 10031
7. Sun JQ, Bartlett RJ (1996) J Chem Phys 104: 8553
8. Liegener CM (1988) J Chem Phys 88: 6999
9. Bogár F, Ladik J (1998) Chem Phys 237: 273
10. Suhai S (1992) Int J Quantum Chem 42: 193
11. Förner W, Knab R, Čižek J, Ladik J (1997) J Chem Phys 106: 10248
12. Abdurahman A, Albrecht M, Shukla A, Dolg M (1998) J Chem Phys 110: 8819
13. Horsch S, Horsch P, Fulde P (1984) Phys Rev B 29: 1870
14. (a) Stoll H (1992) Chem Phys Lett 191: 548; (b) Stoll H (1992) Phys Rev B 46: 6700
15. Gräfenstein J, Stoll H, Fulde P (1993) Chem Phys Lett 215: 610
16. Gräfenstein J, Stoll H, Fulde P (1997) Phys Rev B 55: 13588
17. Albrecht M, Fulde P, Stoll H (2000) Chem Phys Lett 319: 355
18. Tatewaki H (1999) Phys Rev B 60: 3777
19. Shukla A, Dolg M, Stoll H, Fulde P (1996) Chem Phys Lett 262: 213
20. Shukla A, Dolg M, Fulde P, Stoll H (1998) Phys Rev B 57: 1471
21. Shukla A, Dolg M, Fulde P, Stoll H (1999) Phys Rev B 60: 5211
22. Albrecht M, Reinhardt P, Malrieu J-P (1998) Theor Chem Acc 100: 241
23. Igarashi J, Unger P, Hirai K, Fulde P (1994) Phys Rev B 49: 16181
24. Takahashi M, Igarashi J (1996) Phys Rev B 54: 13566
25. Takahashi M, Igarashi J (1999) Phys Rev B 59: 7373
26. Albrecht M, Igarashi J (2001) J Phys Soc Jp A 70: 1035
27. Shirley EL (1998) Phys Rev B 58: 9579
28. Dovesi R, Saunders VR, Roetti C (1992) Computer code Crystal 92. Gruppo di Chimica Teorica, University of Torino and United Kingdom Science and Engineering Research Council Laboratory, Daresbury
29. Fulde P (1995) Electron correlations in molecules and solids, Springer series in solid-state Sciences, vol 100. Springer, Berlin Heidelberg New York
30. Hampel C, Werner H-J (1996) J Chem Phys 104: 6286
31. Reinhardt P, Malrieu J-P (1998) J Chem Phys 109: 7632
32. Poole RT, Jenkin JG, Liesegang J, Leckey RCG (1975) Phys Rev B 11: 5179
33. Poole RT, Liesegang J, Leckey RCG, Jenkin JG (1975) Phys Rev B 11: 5190
34. Piacentini M (1975) Solid State Commun 17: 697
35. O'Bryan HM, Skinner HWB (1940) Proc R Soc Lond Ser A 176: 229
36. Prencipe M, Zupan A, Dovesi R, Aprà E (1995) Phys Rev B 51: 3391